Supplemental file for

Effect of contrasting structural and compositional inheritances on the development of rifting margins

S. Jammes[1], and L. L. Lavier[2]

[1]*Department of geography, Texas State University, San Marcos, Texas 78666 USA,*

[2] *Department of Geological Sciences and Institute for Geophysics, Jackson School of Geosciences, The University of Texas at Austin, Austin, TX 78712, USA*

**E-mails: suzon.jammes@txstate.edu, luc@utig.ig.utexas.edu*

INTRODUCTION

This supplemental file presents the evolution of the models discussed in the paper. For each model, the plastic strain (brittle deformation), the material and the strain rate are plotted for the different phases of deformation. In these models, crustal fabrics are either randomly distributed (reference model, Model 1, Figure S1), horizontal (Model 2, Figure S2), vertical (Model 3, Figure S3) or oblique (30° dip; Model 4, Figure S4). Model 5 is similar to model Model 4 but the crustal fabrics are dipping in the opposite direction. The parameters used in the models (mechanical, thermal, resolution parameters and boundary conditions) are presented in table S1.

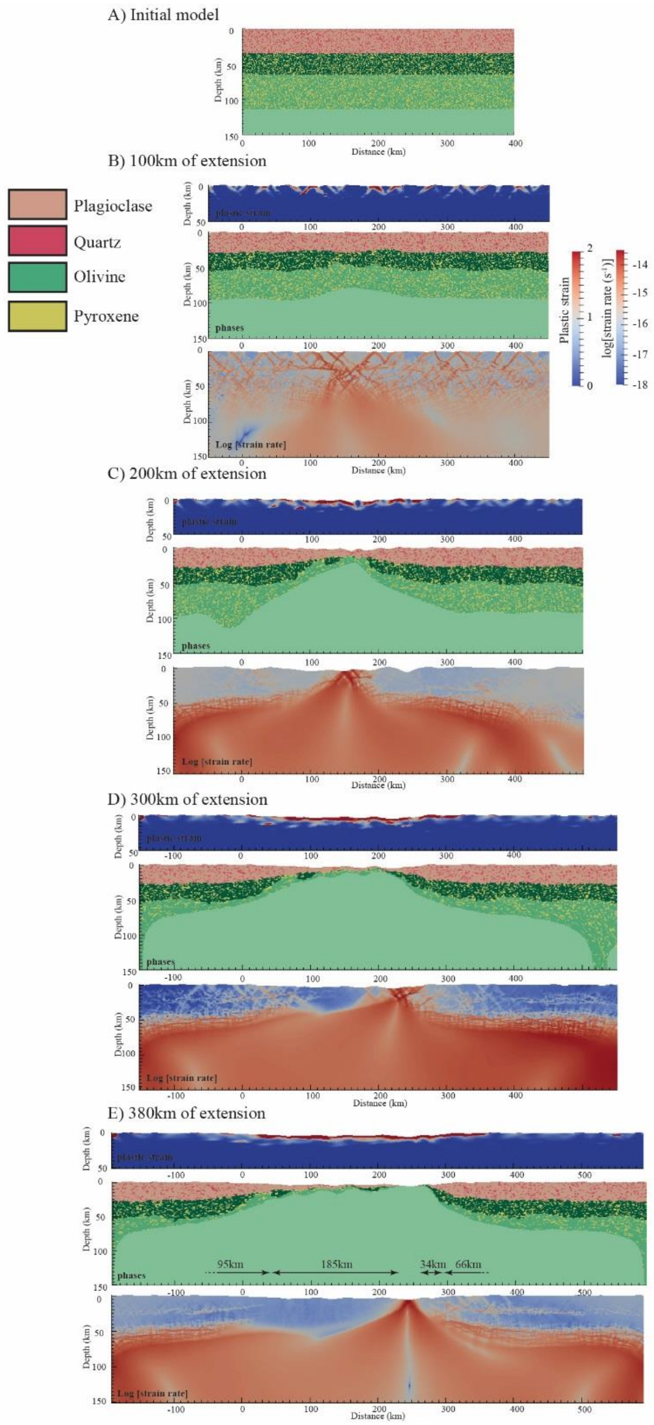

Figure S1 Model 1 evolution with randomly distributed heterogeneities during lithospheric extension (A). The plastic strain (brittle deformation), the material and the strain rate are plotted for the different phases of the deformation: (B) after 100 km, (C) 200 km, (D) 300 km, and (E) 380 km of extension. The length of the necking domain (dashed arrow) and hyperextended domain (plain arrow) are indicated in Figure S1E.

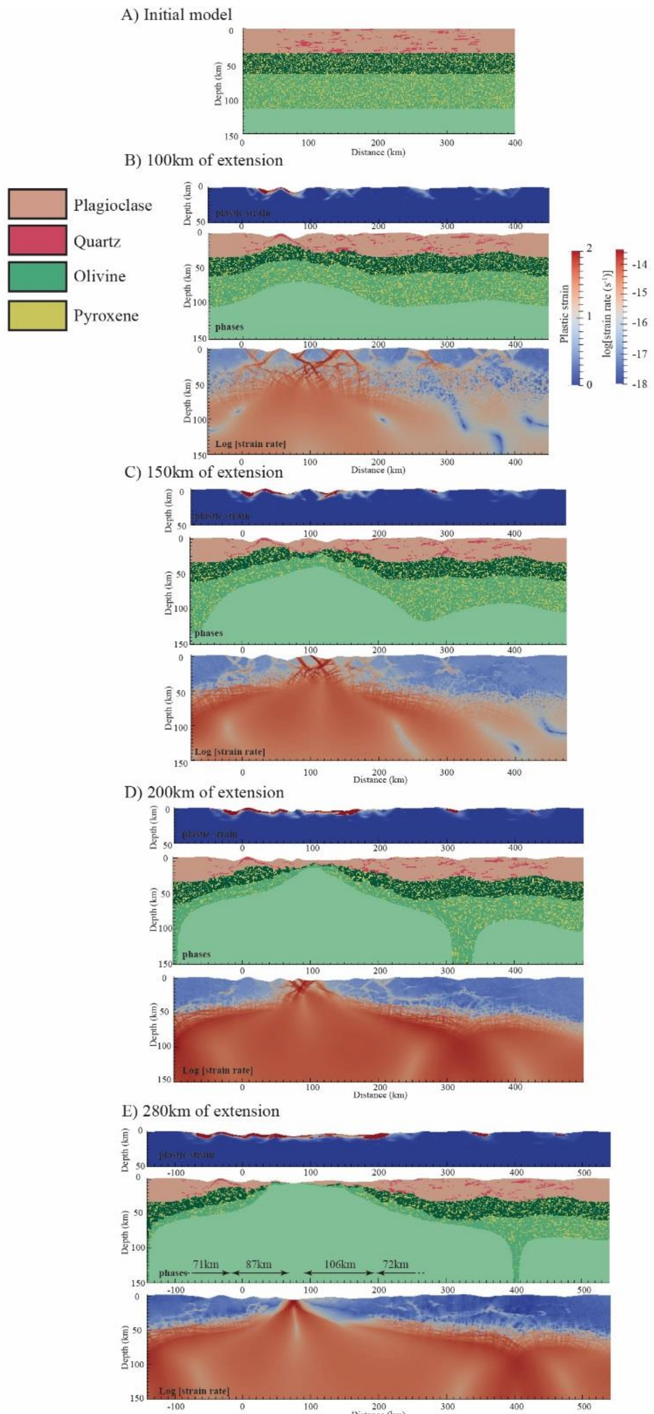

Figure S2. Model 2 with horizontal crustal fabrics during lithospheric extension (A). The plastic strain (brittle deformation), the material and the strain rate are plotted for the different phases of the deformation: (B) after 100 km, (C) 150 km, (D) 200 km, and (E) 280 km of extension. The length of the necking domain (dashed arrow) and hyperextended domain (plain arrow) are indicated in Figure S2E.

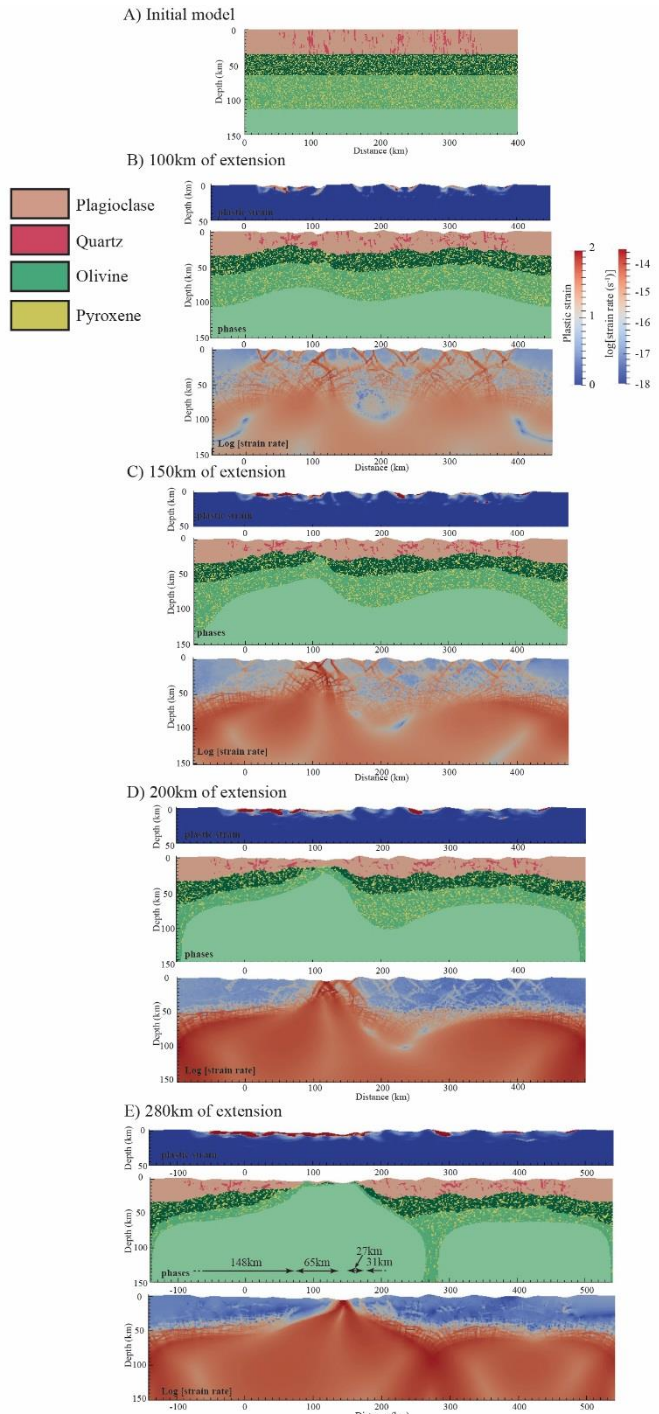

Figure S3. Model 3 with vertical crustal fabrics during lithospheric extension (A). The plastic strain (brittle deformation), the material and the strain rate are plotted for the different phases of the deformation: (B) after 100 km, (C) 150 km, (D) 200 km, and (E) 280 km of extension. The length of the necking domain (dashed arrow) and hyperextended domain (plain arrow) are indicated in Figure S3E.

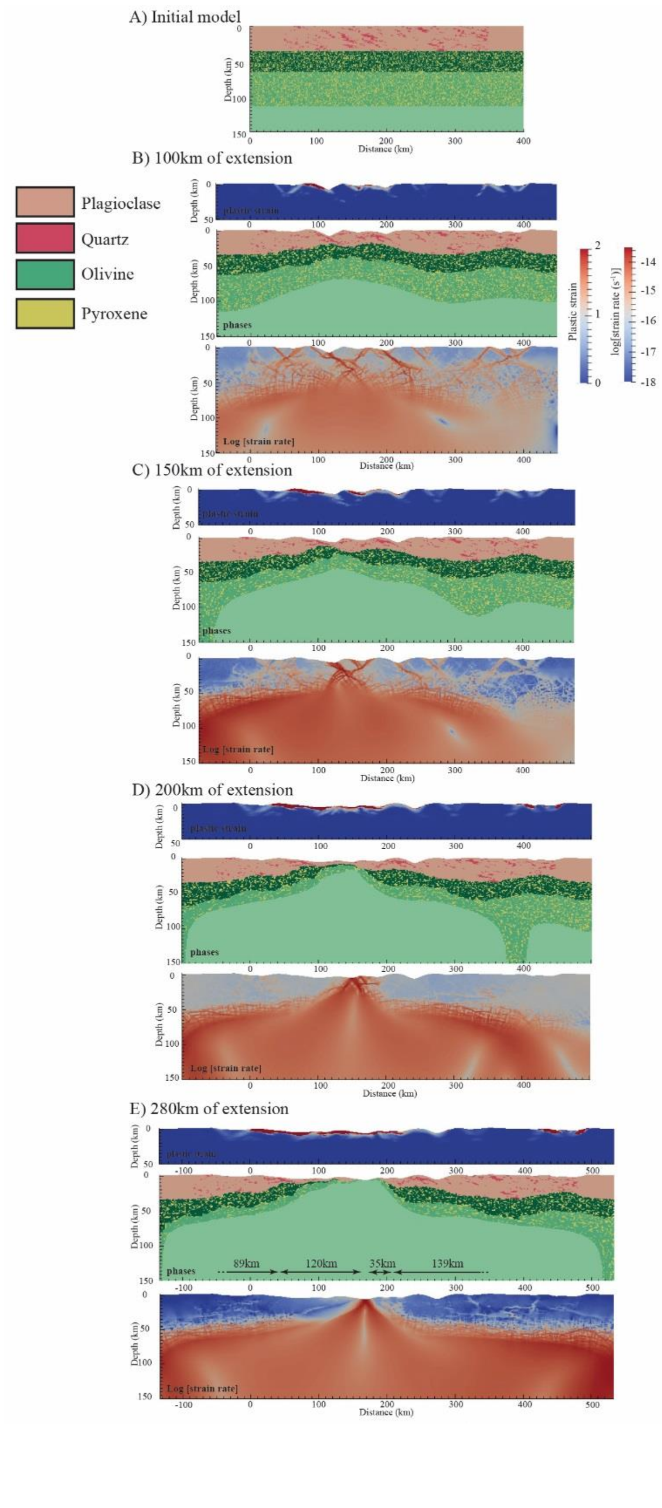

Figure S4. Model 4 with oblique crustal fabrics (30°-dipping toward the right) during lithospheric extension (A). The plastic strain (brittle deformation), the material and the strain rate are plotted for the different phases of the deformation: (B) after 100 km, (C) 150 km, (D) 200 km, and (E) 280 km of extension. The length of the necking domain (dashed arrow) and hyperextended domain (plain arrow) are indicated in Figure S4E.

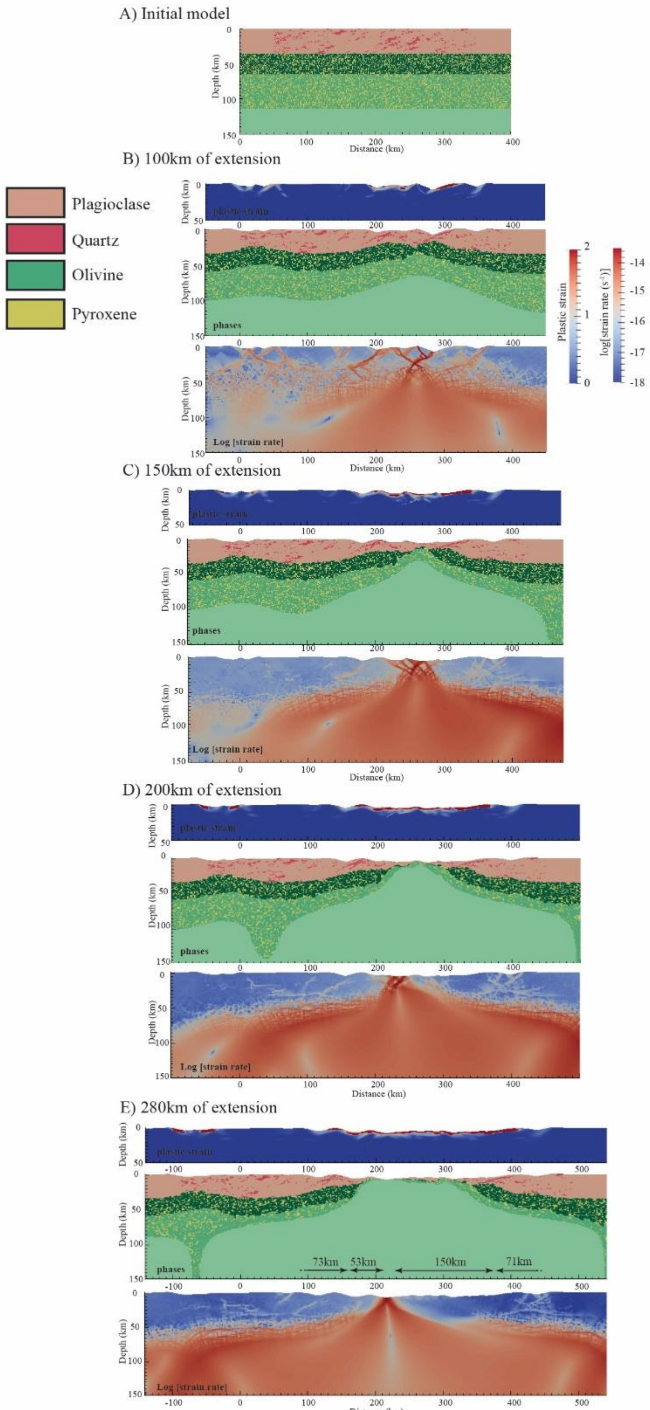

Figure S5. Model 6 with oblique crustal fabrics (30°-dipping toward the left during lithospheric extension (A). The plastic strain (brittle deformation), the material and the strain rate are plotted for the different phases of the deformation: (B) after 100 km, (C) 150 km, (D) 200 km, and (E) 280 km of extension. The length of the necking domain (dashed arrow) and hyperextended domain (plain arrow) are indicated in Figure S5E.

Mechanical parameters			
Friction angle φ	°	30 (15 after strain weakening)	
Cohesion C	Pa	$4\ 10^{7}$-$4\ 10^{6}$	
Universal gas constant R	J.mol-1.°C-1	8.3144	
Flow law Reference A Q n V	 $MPa^{-n}.s^{-1}$ $J.mol^{-1}$ $m^{3}.mol^{-1}$	*Wet quartz* Brace and Kohlstedt, 1980 $5.0\ 10^{2}$ $2.0\ 10^{5}$ 3.3 0	*Plagioclase* Shelton and Tullis, 1981 $3.3\ 10^{-4}$ $2.38\ 10^{5}$ 3.2 0
Ref density ρ	$kg.m^{-3}$	2750	
Flow law Reference A Q n V	 $MPa^{-n}.s^{-1}$ $J.mol^{-1}$ $m^{3}.mol^{-1}$	*Orthopyroxene* Raleigh et al., 1971 $6.07\ 10^{-1}$ $2.0\ 10^{5}$ 2.93 0	*Dry Olivine* Goetze and Poirier, 1978 $7.0\ 10^{4}$ $5.2\ 10^{5}$ 3.0 0
Ref density ρ	$kg.m^{-3}$	3300	
Thermal parameters			
Thermal diffusivity	$m^{2}s^{-1}$	$1\ 10^{-6}$	
Thermal expansion	K^{-1}	$3.0\ 10^{-5}$	
Heat capacity	$J.K^{-1}.kg^{-1}$	1000	
Thermal conductivity	$W.K^{-1}.m^{-1}$	3.3	
Surface Temp.	°C	10	
Moho Temp	°C	500, 600 or 700	
Asthenosphere Temperature	°C	1330	
Basal heat flow	$mW.m^{-2}$	14	
Resolution			
Model domain	km	250 (vertical)*400(horizontal)	
Resolution of the grid	km	1	
Boundary condition			
Boundary velocity	$cm.yr^{-1}$	$V = \pm 1.6 \times 10^{-10}$ m/s or ±0.5 cm/yr	
Upper surface		Free slip	
Basal boundary		Winckler foundation	

Table S1. Mechanical, thermal and resolution parameters and boundary conditions used in the models.